 doi:10.20944/preprints201803.0198.v1

Rhodamine Derivative Functionalized Magnetic Nano-Platform for Cu^{2+} Sensing and Removal

Jiaxin Wang[1], *Shuhan Wang*[1], *Wanqing Tian*[2], *Dong Yao*[2], *Lining Sun*[1], *Liyi Shi*[1] *and Jinliang Liu*[1]*

[1] Research Center of Nano Science and Technology, Shanghai University, 200444, P. R. China

[2] Jingjiang Hospital of Traditional Chinese Medicine, Jiangsu Province, 214500, P. R. China

*To whom the correspondence should be addressed:

Dr. Jinliang Liu

Research Center of Nano Science and Technology, Shanghai University, 200444, China.

Phone: +86-21-66137153

Fax: +86-21-66137153

Email: liujl@shu.edu.cn

 doi:10.20944/preprints201803.0198.v1

Abstract

Pollution caused by copper is one of the key factors of environment contamination. As one of heavy metals, copper is hard to decompose in nature, the biological enrichment of which may lead to severe damage to health. Cu^{2+} detection, thus, possesses a bright application prospect both in environment protection and in human health. In this paper, a dual-functional fluorescence-magnetic composite nano-platform has been designed to sensitively detect, meanwhile capture and remove Cu^{2+} in the solution of water and ethanol (1:1, v/v). The core-shell structure nanoparticle synthesized by using Fe_3O_4 as core and SiO_2 as shell, is covalently bonded with rhodamine derivatives on the silica layer to construct the nano-platform. The emission is increased upon the addition of Cu^{2+}, showing fluorescence turn on effect for the detection, and the limit of detection which was as low as 1.68 nM. Meanwhile, Cu^{2+} ions are captured by the coordination with rhodamine derivatives, and can be removable with the help of magnetic field.

Keywords: Copper detection; magnetic nanoparticle; Rhodamine B derivative; removal

Preprints (www.preprints.org) | NOT PEER-REVIEWED | Posted: 23 March 2018 doi:10.20944/preprints201803.0198.v1

1. Introduction

With the increasing development of social productivity, copper pollution as a representative of heavy metal contamination is getting worse. Copper dust which is made by the weathering of the rocks, mining, metallurgy, machine process, will result in pollution of air, water, soil.[1], [2], [3]. Meanwhile, copper is hard to decompose in nature, the resulting enrichment through food chain may lead to severe damage to health[4], [5]. As an essential trace elements, copper ions if in improper dose[6], is likely to cause human poisoning, illness involves nervous system, digestive system, cardiovascular system, endocrine system etc., the diseases which is known to the majority include Alzheimer, hepatic cirrhosis, leucoderma, skeleton deformity etc.[7], [8], [9], [10]. Therefore, the development of new methods for the detection and removal of copper ions in the environment has attracted a lot of research interests in the past decades.

There are many techniques at present to detect Cu^{2+}, such as Atomic Absorption Spectrometry (AAS), Inductively Coupled Plasma Atomic Emission Spectrometry (ICP-AES), Inductively Coupled Plasma-Mass Spectrometry (ICP-MS), etc[11], [12], [13]. But difficulties still exist in trace analysis, due to the limited sensitivity and detection limits (LOD) of machine. In addition, expensive test cost, large amounts of time in sample preparation, inconvenience for on-site analysis are the stumbling blocks in life and environmental detection of Cu^{2+}. As an effective means, the florescence method has advantages of technical simplicity, high sensitivity, fast response time, non-destructive imaging[14], [15], [16]. In terms of florescence determination, the key procedure is to design and synthesis of fluorescence probe. Lots of fluorescence probes have been developed for detection of Cu^{2+} ions with high sensitivity and selectivity[17], [18], [19]. Among these reports, rhodamine compounds have shown significant advantages over some traditional fluorophores due to their attractive feature such as high photostability, wide wavelength range and high fluorescence quantum yield, and thus become an

Preprints (www.preprints.org) | NOT PEER-REVIEWED | Posted: 23 March 2018 doi:10.20944/preprints201803.0198.v1

extensive research topic in the field of chemistry and biology[20], [21], [22], [23]. However, fluorescence probes with single structure often suffer from some drawbacks, such as low detect efficiencies, difficulties in separation and secondary pollution to environment. Nano-platform which combined the inorganic-organic composite fills the gap by its prominent advantages in complementation and cooperativity in multifunction. As for inorganic composite, magnetic nanoparticles provide us an environmental friendly way of separation and recycle[24], [25], [26]. There are different ways in ions detection and removal based on the functionalized magnetic nano-platform. One of the common ways is adsorption. For instance, Cu^{2+} ions are absorbed by hydroxyl groups from β-cyclodextrin and silane[27]. Another method of ion capture is coordination, for example, adopting 8-hydroxyquinoline-2-carboxylic acid as chelator to coordinate with copper ions[28].

As one kind of famous fluorescent probes, Rhodamine derivatives have advantages on high absorbance, improved fluorescence quantum yield and better photostability. Super-paramagnetic nanomaterial is suitable for magnetic separation and fast enrichment. In this work, a core-shell structured nano-platform which is composed of Fe_3O_4 as core, SiO_2 as shell and rhodamine derivatives as the outer layer has been designed. The synthesized hybrid can realize the fluorescence turn on effect for the Cu^{2+} detection and Cu^{2+} removal with the help of magnetic nanoparticles.

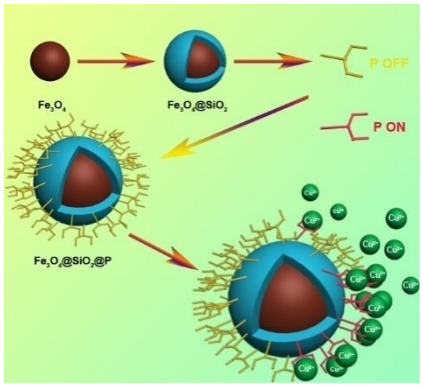

Scheme 1. Schematic illustration of the synthetic procedure of the Fe_3O_4@SiO_2@P and the

Preprints (www.preprints.org) | NOT PEER-REVIEWED | Posted: 23 March 2018 doi:10.20944/preprints201803.0198.v1

proposed sensing and removal mechanism of Fe_3O_4@SiO_2@P towards Cu^{2+} ions.

2. Experimental section

2.1 Materials

1-Octadecene(ODE，technical grade，90%), Oleic acid(OA，technical grade，90%), IGEPAL ®CO-520, Tetraethyl orthosilicate (TEOS, GC, ≥99%) were purchased from Sigma-Aldrich Co. Ltd. (China). Sodium oleate (CP), n-Hexane(AR，97%), Ammonia solution(AR), Salicylaldehyde were obtained from Shanghai Aladdin Chemistry Co., Ltd. (Shanghai, China). Hydrazine hydrate (85%), rhodamine B, （3-isocyanatopropyl）triethoxysilane （GR, 95%）were purchased from J&K Technology Co., Ltd.. Toluene (AR), ）Iron(III)chloride hexahydrate (AR), Anhydrous ethanol (99.7%, AR) were obtained from Sinopharm Chemical Reagent Co. China. All the agents above were used without further purification. Aqueous solution of different ions, such as Cu^{2+}、K^{+}、Ba^{2+}、Co^{2+}、Ca^{2+}、Na^{+}、Mn^{2+}、Mg^{2+}、Ni^{2+} and Hg^{+} were prepared respectively from its chloride salts. Water used during the experiments was deionized water.

2.2 Preparation of Fe_3O_4@ SiO_2

Fe_3O_4 was synthesized through pyrolysis method according to the previous report[29] with some modification. 40 mmol of $FeCl_3$ $6H_2O$ and 40 mmol of sodium oleate were dispersed into 80 mL of ethanol. Then the resulted solution was mixed with 60 mL of deionized water and 140 mL of n-hexane and kept in 70 ℃ for 4 h. After that, 30 mL of deionized water was then added to wash the product, at last the oil phase was gathered and dried overnight. Next, 36 g of the resulting iron-oleat complex was dissolved in 20 mmol of OA, and 200 g of ODE, the mixture were reacted at 320 ℃ for 30 min under Ar. After cooling to the room temperature, the solid product was collected and washed with 20 mL of n-hexane for 3 times. Finally, the nanocrystals were dispersed in n-hexane (30 mg/mL) for

Preprints (www.preprints.org) | NOT PEER-REVIEWED | Posted: 23 March 2018 doi:10.20944/preprints201803.0198.v1

storage.

Reversed-phase microemulsion method was used in forming silica layer outside of the Fe_3O_4. 250 μL of Fe_3O_4 dispersion was diluted with 10 mL of n-hexane. 50 μL of CO-520 was added while vigorous stirring, then kept at the same condition continuously for 30 min. Next, 2 μL of TEOS was added slowly. Afterwards, 10 μL of ammonia solution was added and the mixture was stirred continuously for 20 h. The resulting products were washed using ethanol as precipitant via centrifugal separation for 3 times. At last, Fe_3O_4@SiO_2 was obtained and dispersed in 5mL of ethanol at 4 ℃.

2.3 Preparation of Fe_3O_4@ SiO_2@P

The rhodamine derivative (P for short) was synthesized according to our previous article[30]. 60 mg of Fe_3O_4@SiO_2 nanoparticles was re-dispersed in 20 mL of toluene, and then the solution was heated to 80 ℃. 20 μL of (3-isocyanatopropyl) triethoxysilane was added by drops and the temperature was kept at 110 ℃ for 12 h. After that, P (120 mg) distributed in 1 mL of toluene was injected into the reactant rapidly, then, kept it at 110 ℃ for another 12 h. After cooling down to room temperature, Fe_3O_4@SiO_2@P was collected via centrifugation and washed with alcohol for three times. Finally, Fe_3O_4@SiO_2@P was dispersed in 5 mL of ethanol and sealed for storage at 4 ℃ for further use.

2.4 Characterization

The morphology features of nanoparticles were observed by transmission electron microscope (TEM, JEM-200CX) at 200 kV. Vibrating Sample Magnetometer (VSM, 7407; lakeshore) was used for evaluating the magnetic properties at room temperature. Fourier transform infrared (FTIR, AVATAR370, Nicolet) spectroscopy was to analyze functional groups from synthesized materials. Structure analysis of organic molecules was performed by Fourier superconducting nuclear magnetic resonance spectrometer (AVANCE 500 MHz, BRUKER), using tetramethylsilane (TMS) as an

Preprints (www.preprints.org) | NOT PEER-REVIEWED | Posted: 23 March 2018 doi:10.20944/preprints201803.0198.v1

internal standard. To detect the actual ion concentrations, inductively coupled plasma atomic emission spectroscopy (ICP-AES, HORIBA JOBIN YVONSAS) was employed. Fluorescent properties were determined by a LS-55 spectrophotometer. The excitation wavelength was 520 nm, and the emissions were collected from 470 to 750 nm. Absorption spectrum was detected by UV-VIS Spectrophotometer (UV-2600; SHIMADZU). All the measurements mentioned above were conducted at room temperature.

2.5 Cu^{2+} response and removal

A stock solution of Fe_3O_4@SiO_2@P (10 mg/mL) was prepared in the solution of water and ethanol (1:1, v/v). Stock solutions of the metal ions (0.1 M) were prepared in deionized water. Titration experiments were performed by adding Cu^{2+} solution incrementally to a solution of Fe_3O_4@SiO_2@P (2.5 mL). For the selectivity experiments, the test samples were prepared by adding appropriate amounts (100 equiv.) of metal ions solution to 2.5 mL of a solution of Fe_3O_4@SiO_2@P. In competition experiments, Cu^{2+} was added to the solutions containing Fe_3O_4@SiO_2@P and other metal ions of interest. In Cu^{2+} removal experiments (three parallels), Cu^{2+} (1 mL, 0.1 M) was added in Fe_3O_4@SiO_2@P (2.5 mL) and dispersed evenly. With magnet treatment, the resulted supernate was collected respectively after 5 min and 10 min. All solutions were stirred for 3 min at room temperature and then used for the spectroscopic test.

3. Results and Discussions

Preprints (www.preprints.org) | NOT PEER-REVIEWED | Posted: 23 March 2018 doi:10.20944/preprints201803.0198.v1

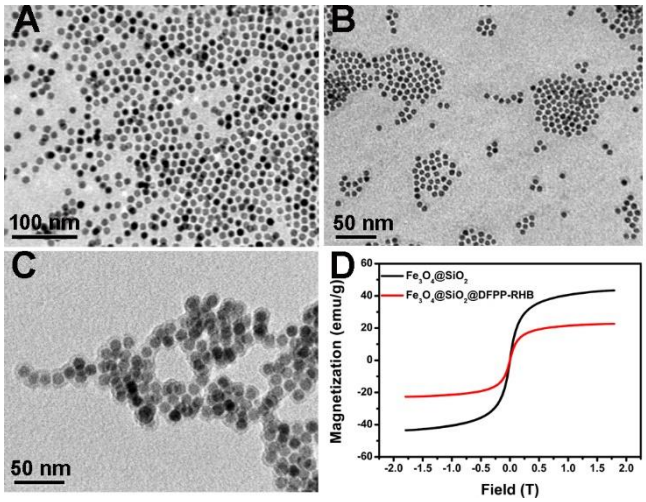

Figure 1. The TEM images of (A) Fe_3O_4, (B) Fe_3O_4@SiO_2, (C) Fe_3O_4@SiO_2@P. (D) magnetic hysteresis loop of Fe_3O_4@SiO_2 (black line) and Fe_3O_4@SiO_2@P (red line).

3.1 Morphology and structure characterization

Fe_3O_4 nanoparticle was designed as the core, and its intrinsic magnetism was the critical factor for separation and removal of Cu^{2+} with external magnetic field. As **Figure 1A** showed, Fe_3O_4 was uniform and monodisperse and the measured diameter was 9.88 ±0.79 nm. By utilizing reversed-phase microemulsion method, solid silica was coated on the surface of Fe_3O_4 via TEOS hydrolysis-condensation reaction, the obtained Fe_3O_4@SiO_2 possessed regular morphology with the average diameter was 21.63 ±1.57 nm, and the average thickness of silica layer was about 5 nm measured from the TEM images (**Figure 1B)**. The magnetic nano-platform Fe_3O_4@SiO_2@P was finally achieved by the nucleophilic addition reaction between the amino group of (3-isocyanatopropyl) triethoxysilane and the hydroxyl group of P. Some aggregation appeared after dye loading **(Figure 1C**), this is mainly because of the hydrophobic property of the organic probe molecule P. The saturated magnetization of Fe_3O_4@SiO_2 was 43.451 emu/g, as shown in Figure 1D, while after combine with organic probe molecule, the value of which was decreased to 22.669 emu/g. It's suggested that two outer layers' nonmagnetic nature lead to the decrease of maximun saturation magnetizations.

Preprints (www.preprints.org) | NOT PEER-REVIEWED | Posted: 23 March 2018 doi:10.20944/preprints201803.0198.v1

Fourier transform infrared spectroscopy (FTIR) of Fe_3O_4@SiO_2 and Fe_3O_4@SiO_2@P was carried out in order to testify the successful loading of P. As **Figure 2** showed, FTIR of Fe_3O_4@SiO_2 exhibited two characteristic bands of silica layer. Peak at 1094 cm^{-1} was attributed to Si-O-Si symmetric stretching vibrations, and peak at 562 was assigned to Si-O symmetric stretching vibrations. The spectrum of Fe_3O_4@SiO_2@P showed C=C symmetric stretching vibrations at 1616 cm^{-1}, 1514 cm^{-1}, 1461 cm^{-1}, which belonged to benzene ring. Also, C=O stretching vibration at 1715 cm^{-1} appeared, thus, it's could be concluded that covalent bonding existed between P and silica.

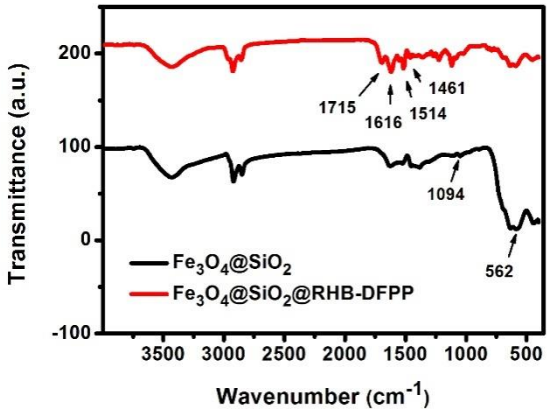

Figure 2. FTIR spectra of Fe_3O_4@SiO_2 and Fe_3O_4@SiO_2@P.

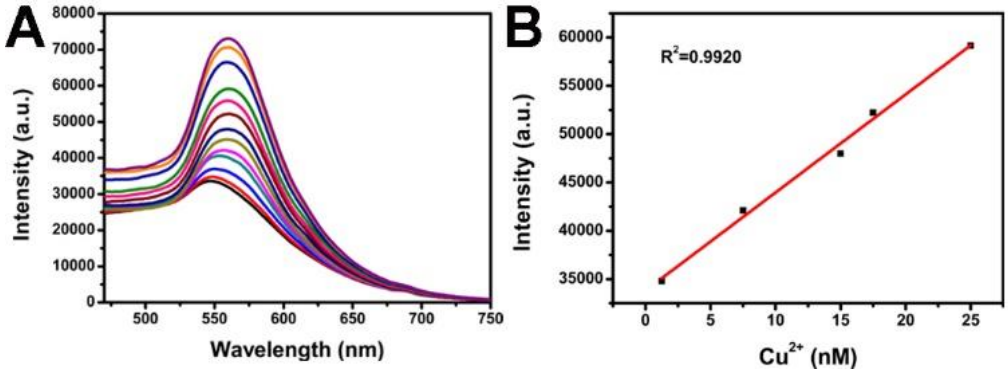

Figure 3. The emission spectra (A) of Fe_3O_4@SiO_2@P upon various concentrations of Cu^{2+} (λ_{ex}=520nm); the linear fitting of florescence intensities at peak of 550 nm towards the concentrations of Fe_3O_4@SiO_2@P (B).

Sensing and capture of Cu^{2+}

Preprints (www.preprints.org) | NOT PEER-REVIEWED | Posted: 23 March 2018 doi:10.20944/preprints201803.0198.v1

The ions-responsive mechanism was achieved due to the well-known equilibrium between the non-fluorescent spirolactam and the fluorescent ring-opened amide of rhodamine. The emission spectrum of Fe_3O_4@SiO_2@P upon various concentrations of Cu^{2+} is shown in Figure 3A. Under the excitation at 520 nm, an emission band centered at 552 nm appears and the intensity increases evidently with the Cu^{2+} concentration increased gradually. This indicates the ring-open process of the rhodamine B unit in P happened. A linear correlation between the emission intensity and concentration of Cu^{2+} in the range of 0-25 nM can be observed (**Figure 3B**). The limit of detection (LOD) was calculated as low as 1.68 nM by the following formula LOD = $3S_0/S$ (where S_0 is the standard deviation of the blank measurements, S is the slope of the calibration curve, 3 is the factor at the 99% confidence level), suggesting the high sensitivity of the nano-platform for detecting Cu^{2+}.

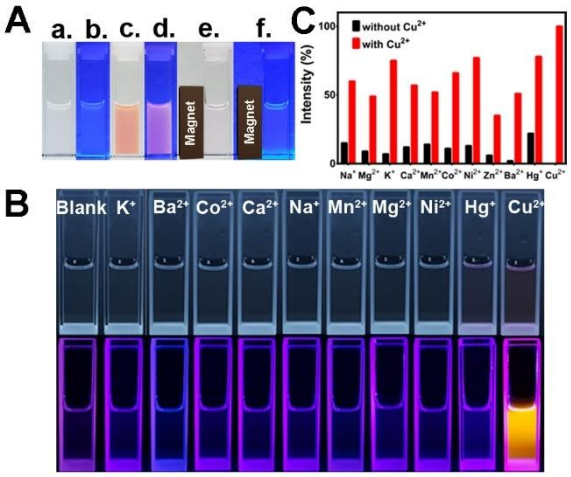

Figure 4. (A) photos of Fe_3O_4@SiO_2@P with(c-f)/without(a, b) Cu^{2+} under daylight(a, c, e)/UV(b, d, f), using magnet(e, f)/no magnet(a-d); (B) photos of Fe_3O_4@SiO_2@P added with various metal ions respectively; (C) ions competition experiment of Fe_3O_4@SiO_2@P in the presense of 2.5 μM Cu^{2+}, upon the back ground of various metal ions (2.5 μM).

Benefits from the intrinsic structure of P and the magnetic properties of Fe_3O_4, the nano-platform can realize the fluorescent detection of Cu^{2+} with naked eyes and removal of Cu^{2+} with the help of

Preprints (www.preprints.org) | NOT PEER-REVIEWED | Posted: 23 March 2018 doi:10.20944/preprints201803.0198.v1

magnetic field. As shown in Figure 4A, before the addition of Cu^{2+}, the hybrid nano-platform was light brown color and non-florescent. When Cu^{2+} added, the hydrazide group and O-acyl hydroxylamines bonded with Cu^{2+}, and thus lead to the opening of the spirolactam ring in P molecule. The resulting conjugate π-bond facilitate the enhancement of florescence intensity at 550 nm, also, photoinduced electron transfer (PET) was blocked, thus it turned into pink color[31], [32], [33]. The Cu^{2+} removal effect of the nano-platform were shown in Figure 4A (e,f), we can see that, after a few seconds, the nano-platform together with Cu^{2+} gathered to the side of cuvette with magnetic felid, the removal efficiency of Cu^{2+} was 75% calculated from ICP-AES results. Furthermore, the selective experiments were done to demonstrate the nano-platform can detect Cu^{2+} exclusively over other metal ions. As shown in Figure 4B. there was nearly no color change upon the introduction of other metal ions, including K^{+}, Ba^{2+}, Co^{2+}, Ca^{2+}, Na^{+}, Mn^{2+}, Mg^{2+}, Ni^{2+}, and Hg^{2+}. Additionally, competition experiments were further carried out by adding Cu^{2+} to the solutions containing both nano-platform and the metal ions of interest. As shown in Figure 4C, these co-existent ions had negligible interference on Cu^{2+} sensing even the competitive ions were present at high concentrations.

Conclusions

In brief, a dual-functional hybrid nano-platform Fe_3O_4@SiO_2@P had been successfully prepared. This nano-platform was composited by the Fe_3O_4 as the core to endow it with magnetism, SiO_2 as one thin layer to bridge the inorganic-organic composite together, and rhodamine derivative P as the outer layer for fluorescent sensing of Cu^{2+}. Benefits from the intrinsic structure of P and the magnetic properties of Fe_3O_4, the nano-platform can realize the fluorescent detection of Cu^{2+} with naked eyes and removal of Cu^{2+} with the help of magnetic field. This nano-platform was featured of simple operation, uniform particle size, structural stability, and excellent magnetic responsibility, and thus can be used for the cell

 doi:10.20944/preprints201803.0198.v1

imaging of Cu^{2+} or removal of Cu^{2+} from the environmental pollution.

Acknowledgements

We are grateful for the financial support from the National Natural Science Foundation of China (Grant Nos. 21201117, 21231004), Medical Research Project of Jiangsu Provincial Commission of Health and Family Planning (NO. Z201624).

References

1. Dragovic, S.; Mihailovic, N., Analysis of mosses and topsoils for detecting sources of heavy metal pollution: multivariate and enrichment factor analysis. *Environ Monit Assess* **2009,** 157, (1-4), 383-390.
2. Huber, M.; Welker, A.; Helmreich, B., Critical review of heavy metal pollution of traffic area runoff: Occurrence, influencing factors, and partitioning. *Sci Total Environ* **2016,** 541, 895-919.
3. Ding, Q.; Cheng, G.; Wang, Y.; Zhuang, D. F., Effects of natural factors on the spatial distribution of heavy metals in soils surrounding mining regions. *Sci Total Environ* **2017,** 578, 577-585.
4. Nesterkova, D. V.; Vorobeichik, E. L.; Reznichenko, I. S., The effect of heavy metals on the soil-earthworm-European mole food chain under the conditions of environmental pollution caused by the emissions of a copper smelting plant. *Contemp Probl Ecol+* **2014,** 7, (5), 587-596.
5. Dallinger, R.; Wieser, W., The flow of copper through a terrestrial food chain. *Oecologia* **1977,** 30, (3), 253-264.
6. Prohaska, J. R., Impact of copper deficiency in humans. *Ann Ny Acad Sci* **2014,** 1314, 1-5.
7. Jomova, K.; Baros, S.; Valko, M., Redox active metal-induced oxidative stress in biological systems. *Transit Metal Chem* **2012,** 37, (2), 127-134.
8. Suttle, N. F., Copper Imbalances in Ruminants and Humans: Unexpected Common Ground. *Adv Nutr* **2012,** 3, (5), 666-674.
9. Djoko, K. Y.; Paterson, B. M.; Donnelly, P. S.; McEwan, A. G., Antimicrobial effects of copper(II) bis(thiosemicarbazonato) complexes provide new insight into their biochemical mode of action. *Metallomics* **2014,** 6, (4), 854-863.

10. Wijmenga, C.; Klomp, L. W. J., Molecular regulation of copper excretion in the liver. *P Nutr Soc* **2004,** 63, (1), 31-39.

11. Zhuravlev, A.; Zacharia, A.; Arabadzhi, M.; Turetta, C.; Cozzi, G.; Barbante, C., Comparison of analytical methods: ICP-QMS, ICP-SFMS and FF-ET-AAS for the determination of V, Mn, Ni, Cu, As, Sr, Mo, Cd and Pb in ground natural waters. *Int J Environ an Ch* **2016,** 96, (4), 332-352.

12. Tu, Y. G.; Zhao, Y.; Xu, M. S.; Li, X.; Du, H. Y., Simultaneous Determination of 20 Inorganic Elements in Preserved Egg Prepared with Different Metal Ions by ICP-AES. *Food Anal Method* **2013,** 6, (2), 667-676.

13. Li, Z. H.; Chen, J. X.; Liu, M. S.; Yang, Y. L., Supramolecular solvent-based microextraction of copper and lead in water samples prior to reacting with synthesized Schiff base by flame atomic absorption spectrometry determination. *Analytical Methods* **2014,** 6, (7), 2294-2298.

14. Zhou, Y.; Xu, Z.; Yoon, J., Fluorescent and colorimetric chemosensors for detection of nucleotides, FAD and NADH: highlighted research during 2004-2010. *Chemical Society reviews* **2011,** 40, (5), 2222-2235.

15. Kim, H. N.; Guo, Z. Q.; Zhu, W. H.; Yoon, J.; Tian, H., Recent progress on polymer-based fluorescent and colorimetric chemosensors. *Chemical Society reviews* **2011,** 40, (1), 79-93.

16. Kim, H. N.; Ren, W. X.; Kim, J. S.; Yoon, J., Fluorescent and colorimetric sensors for detection of lead, cadmium, and mercury ions. *Chemical Society reviews* **2012,** 41, (8), 3210-3244.

17. Lu, W. J.; Gao, Y. F.; Jiao, Y.; Shuang, S. M.; Li, C. Z.; Dong, C., Carbon nano-dots as a fluorescent and colorimetric dual-readout probe for the detection of arginine and Cu2+ and its logic gate operation. *Nanoscale* **2017,** 9, (32), 11545-11552.

18. Shu, Q.; Liu, M. L.; Ouyang, H.; Fu, Z. F., Label-free fluorescent immunoassay for Cu2+ ion detection based on UV degradation of immunocomplex and metal ion chelates. *Nanoscale* **2017,** 9, (34), 12302-12306.

19. Liu, Z.; He, W.; Pei, M. S.; Zhang, G. Y., A fluorescent sensor with a detection level of pM for Cd2+ and nM for Cu2+ based on different mechanisms. *Chemical communications* **2015,** 51, (75), 14227-14230.

20. Huang, Y. L.; Walker, A. S.; Miller, E. W., A Photostable Silicon Rhodamine Platform for Optical Voltage Sensing. *Journal of the American Chemical Society* **2015,** 137, (33), 10767-

10776.

21. Boyarskiy, V. P.; Belov, V. N.; Medda, R.; Hein, B.; Bossi, M.; Hell, S. W., Photostable, amino reactive and water-soluble fluorescent labels based on sulfonated rhodamine with a rigidized xanthene fragment. *Chem-Eur J* **2008,** 14, (6), 1784-1792.
22. Liu, J.; Sung, Y. Q.; Zhang, H. X.; Shi, H. P.; Shi, Y. W.; Guo, W., Sulfone-Rhodamines: A New Class of Near-Infrared Fluorescent Dyes for Bioimaging. *ACS applied materials & interfaces* **2016,** 8, (35), 22953-22962.
23. Hanczyc, P.; Sznitko, L., Laser-Induced Population Inversion in Rhodamine 6G for Lysozyme Oligomer Detection. *Biochemistry-Us* **2017,** 56, (22), 2762-2765.
24. Zhang, L. Y.; Zhao, Q.; Liang, Z.; Yang, K. G.; Sun, L. L.; Zhang, L. H.; Zhang, Y. K., Synthesis of adenosine functionalized metal immobilized magnetic nanoparticles for highly selective and sensitive enrichment of phosphopeptides. *Chemical communications* **2012,** 48, (50), 6274-6276.
25. Li, H.; Shan, Y. H.; Qiao, L. Z.; Dou, A.; Shi, X. Z.; Xu, G. W., Facile Synthesis of Boronate-Decorated Polyethyleneimine-Grafted Hybrid Magnetic Nanoparticles for the Highly Selective Enrichment of Modified Nucleosides and Ribosylated Metabolites. *Analytical chemistry* **2013,** 85, (23), 11585-11592.
26. Hu, Z. Y.; Zhao, L.; Zhang, H. Y.; Zhang, Y.; Wu, R. A.; Zou, H. F., The on-bead digestion of protein corona on nanoparticles by trypsin immobilized on the magnetic nanoparticle. *J Chromatogr A* **2014,** 1334, 55-63.
27. Zhang, Y.; Wang, W.; Li, Q.; Yang, Q.; Li, Y.; Du, J., Colorimetric magnetic microspheres as chemosensor for Cu(2+) prepared from adamantane-modified rhodamine and beta-cyclodextrin-modified Fe3O4@SiO2 via host-guest interaction. *Talanta* **2015,** 141, 33-40.
28. Cui, Z.; Bu, W.; Fan, W.; Zhang, J.; Ni, D.; Liu, Y.; Wang, J.; Liu, J.; Yao, Z.; Shi, J., Sensitive imaging and effective capture of Cu(2+): Towards highly efficient theranostics of Alzheimer's disease. *Biomaterials* **2016,** 104, 158-67.
29. Park, J.; An, K.; Hwang, Y.; Park, J. G.; Noh, H. J.; Kim, J. Y.; Park, J. H.; Hwang, N. M.; Hyeon, T., Ultra-large-scale syntheses of monodisperse nanocrystals. *Nature materials* **2004,** 3, (12), 891-5.
30. Meng, X.; Xu, Y.; Liu, J.; Sun, L.; Shi, L., A new fluorescent rhodamine B derivative as an

 doi:10.20944/preprints201803.0198.v1

"off–on" chemosensor for Cu2+with high selectivity and sensitivity. *Anal. Methods* **2016,** 8, (5), 1044-1051.

31. Virginie, D. F., Ford; Anthony W. Czarnik, A_Long-Wavelength Fluorescent Chemodosimeter Selective for Cu(II) Ion in Water. *Journal of the American Chemical Society* **1997,** 119, (31), 7386-7387.
32. Li, j. H., Q.; Zeng, Y.; Yu, X.; Pan, Z., Rhodamine-Based Fluorescent Probes for Cations. *Process In Chemistry* **2012,** 24, (5), 823-833.
33. Yuan, Y. T., M.; Feng, F.; Meng, S.; Bai, Y., Rhodamine-Based Cations Fluorescent Probes. *Process In Chemistry* **2010,** 22, (10), 1929-1939.